Published in IET Communications
Received on 18th June 2009
Revised on 1st September 2009
doi: 10.1049/iet-com.2009.0381

ISSN 1751-8628

Optimal power allocation and power control for VBLAST systems with *M*-ary modulations

H.-Y. Chen[1] *C.-H. Chuang*[1] *P.-C. Yeh*[1] *S.A. Zummo*[2]

[1]*Department of Electrical Engineering and Graduate Institute of Communication Engineering, National Taiwan University, Taipei, Taiwan*
[2]*Electrical Engineering Department, KFUPM, Dhahran 31261, Saudi Arabia*
E-mail: pcyeh@cc.ee.ntu.edu.tw

Abstract: In this study, the authors propose the optimal power allocation scheme that minimises the symbol error probability (SER) of vertical Bell Laboratories layered space-time (VBLAST) systems using *M*-ary modulations. The essence of the power allocation is to intentionally cause different received power from each layer at the receiver. By judiciously allocating the transmitting power to the layers, the performance of the successive interference cancelation at the receiver can be significantly improved. The exact SER of the VBLAST systems with non-uniform power allocation is analysed for the Rayleigh fading case. The SER is minimised to determine the optimal power allocation pattern for the VBLAST systems with *M*-ary modulations. Simulations show that our SER analysis is accurate and the proposed power allocation scheme significantly improves the performance of the VBLAST systems in fast fading environments by 3.5–4 dB. The work is applied to the power control of VBLAST systems in slow fading environments. Significant SNR gains of 8.5–10 dB are observed in the numerical experiments. It is also observed that the proposed optimal power allocation scheme can effectively reduce the SER variation among the layers.

1 Introduction

The multi-input multi-output (MIMO) architecture proposed by Foschini [1], also known as Bell Laboratories layered space-time (BLAST) architecture, is well known for its high spectral efficiency achieved by using multiple antennas. Several types of BLAST systems have been proposed, and the most popular one is the vertical BLAST (VBLAST) [2]. In the VBLAST architecture, multiple data streams are transmitted over the multiple transmit antennas (layers) simultaneously, which are practically detected at the receiver using successive interference cancelation (SIC) to achieve good system performance at moderate complexity.

In this paper, we consider the power allocation/control of VBLAST systems using M-ary modulation schemes in both fast and slow Rayleigh fading environments. In the literature, the analysis of VBLAST systems with power allocation is often conducted under the non-realistic assumption of perfect interference cancelation during the detection. In [3], the BER of ZF-SIC VBLAST systems given the channel realisations is derived, and the average BER under Rayleigh fading is derived in [4]. The power allocation schemes are then designed in [3, 5] based on the BER analysis. Since the error propagation effect among the layers resulted from the imperfect interference cancelation can severely degrade the VBLAST performance, the power allocation schemes derived in these works under the assumption of perfect interference cancelation are thus not optimal in reality. In [6], the probability of at least one error is derived for $2 \times N$ ZF-SIC VBLAST with BPSK. The probability equals 1 minus the probability of both layers being correctly detected. So strictly speaking, the analysis does not consider the effect of error propagation among the layers either. In [7], the perfect interference cancelation assumption is not applied. However, the power allocation scheme is obtained purely from simulations.

In [8, 9], the optimal power allocation of the VBLAST system using QR-based detection is derived analytically with the error propagation among the layers taken into account. The QR-based detector detects the layers by applying QR factorisation to the MIMO channel matrix. It is known that the QR-based detection suffers more from the error propagation than other approaches [9]. Due to the better performance of the ZF-SIC detection compared to the QR-based detection [10], the performance analysis and the optimal power allocation of ZF-SIC VBLAST systems with error propagation considered are further studied in [11–13], yet these works only focus on the BPSK modulation case. Conceptually the ideas in these papers can be extended for modulations of higher orders. However, such an extension is not straightforward due to the complexity of characterising the error propagation effects among the layers, which results in significantly more bulky expressions as authors commented in [13].

In this paper, we analyse the error probability of the ZF-SIC VBLAST systems using M-ary modulations over fast and slow Rayleigh fading channels. In the fast fading case, the channel varies every symbol duration; whereas in the slow fading case, the channel remains constant for more than one symbol period (at least two symbol periods). The symbol error probability (SER) is analysed for each layer (sub-stream) by taking into accounts the error propagation effect from the previously detected layers. Based on the SER analysis, we search for the optimal power allocation that minimises the average SER over all layers. Simulation results show that our power allocation scheme significantly improves the SER with signal-to-noise ratio (SNR) gains around 3.5–4 dB. It is also observed that the proposed scheme is very effective in reducing the SER variation among the layers so that each layer can provide nearly equal reliability for data transmissions.

On the other hand, it is observed from our work that the optimal power allocation varies as SNR changes. Hence the resulting work can be applied to the power control of VBLAST systems in practical system deployments. The optimal and the suboptimal power control schemes are then proposed for VBLAST systems in slow fading environments. The former requires the receiver to feedback the estimated channel matrix to the transmitter to determine the optimal power allocation; whereas the latter only feedbacks simple information regarding the ordering of the post-detection SNR of the layers. Numerical results show that our optimal power control scheme for a 16-QAM VBLAST system is able to achieve SNR gain up to 10 dB whereas the gain of the suboptimal scheme is around 8.5 dB. It is noted that the significant SNR gain of the optimal scheme comes with the cost of the substantial feedback overhead of the estimated channel matrix. The suboptimal scheme only requires simple feedback of the post-detection SNR which makes it more suitable for application in practical system designs.

The remainder of this paper is organised as follows. In Section 2, the system model and the detection process of VBLAST systems are described. In Section 3, the SER of a VBLAST system with power allocation over fast and slow fading channels is derived. In Section 4, we search for the optimal power allocation scheme for VBLAST systems. In Section 5, we propose two power allocation schemes for the slow fading environments. Numerical results are presented in Section 6. Finally, conclusions are given in Section 7.

2 System model

A typical VBLAST system is shown in Fig. 1, which consists of n_T transmit and n_R receive antennas. The $n_R \times n_T$ channel matrix is composed of samples drawn from Rayleigh fading random processes, which remain constant during the transmission of a whole data block. The channel matrix can be denoted as follows

$$\boldsymbol{H} = \begin{bmatrix} h_{11} & \cdots & h_{1n_T} \\ \vdots & \ddots & \vdots \\ h_{n_R 1} & \cdots & h_{n_R n_T} \end{bmatrix} \quad (1)$$

where h_{ij} denotes the complex channel gain from the jth transmit antenna to the ith receive antenna. Since the signals in a scattering environment received at each receive antenna appear to be uncorrelated, it is assumed that $\{h_{ij}\}$ are independent and identically-distributed (i.i.d.) complex Gaussian random variables with zero-mean and $E[|h_{ij}|^2] = 1$.

The modulation schemes considered are M-PSK and M-QAM. The data stream from a single user is demultiplexed

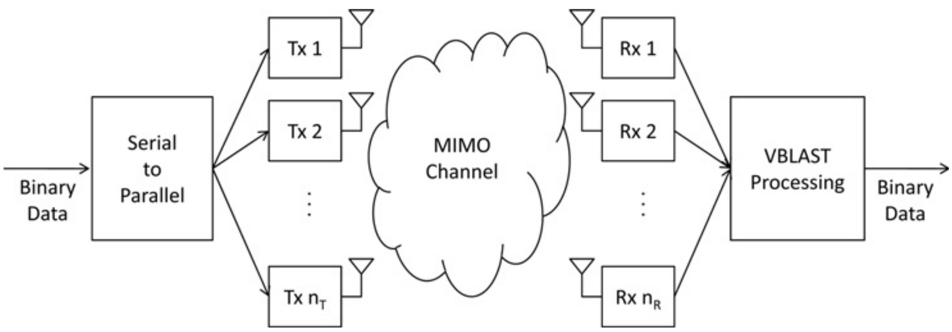

Figure 1 *VBLAST system architecture*

into n_T sub-streams, where the jth sub-stream is transmitted through the jth transmit antenna. All transmit antennas transmit at the same frequency band simultaneously, which results in the high spectral efficiency of VBLAST systems. Denote the vector of the transmit symbols by $\boldsymbol{x} = [x_1, x_2, \ldots, x_{n_T}]^T$, where x_j is the symbol of the jth sub-stream; and define r_i as the received signal and n_i as the white Gaussian noise at the ith receive antenna. Note that $\{n_i\}$ are complex Gaussian distributed with zero mean and variance N_0. The received signal vector can be expressed as

$$\boldsymbol{r} = \boldsymbol{Hx} + \boldsymbol{n} \tag{2}$$

where $\boldsymbol{r} = [r_1, r_2, \ldots, r_{n_R}]^T$ and $\boldsymbol{n} = [n_1, n_2, \ldots, n_{n_R}]^T$.

The power allocation pattern for the VBLAST system is characterised by $\boldsymbol{K} = [K_1, K_2, \ldots, K_{n_T-1}]$ where K_i is defined as the transmit power ratio of the ith layer to the sum of layer $i+1, \ldots, n_T$. Since the symbol power is proportional to the symbol energy, $\{K_i\}$ satisfy

$$E_i = K_i \cdot \sum_{j=i+1}^{n_T} E_j, \quad i = 1, 2, \ldots, n_T - 1 \tag{3}$$

with E_i denoting the transmit energy of the ith sub-stream, that is, $E_i = E[|x_i|^2]$, where $E[\cdot]$ denotes the expectation operator. For fair comparison among different energy allocation patterns, E_i must satisfy the energy conservation constraint, $E_T = \sum_{i=1}^{n_T} E_i = n_T E_s$, where E_s denotes the average transmit energy per modulation symbol.

The receiver is assumed to have perfect channel state information (CSI). In detecting the VBLAST system, we need to estimate the vector $\boldsymbol{x}$ given $\boldsymbol{r}$ and $\boldsymbol{H}$ in (2). The detection proceeds sequentially in layers using the ZF-SIC receiver. To detect the symbol of the ith layer, the receiver first nulls the interference from other layers using the ZF scheme and then makes the decision on the symbol. After that, the receiver applies SIC to cancel the contribution of the detected layer from the received signal vector to decrease the interference affecting layers yet to be detected. Similar procedures are applied to the remaining layers. The general form of the modified received symbol vector after the detection of the ith layer is

$$\begin{aligned} \boldsymbol{r}^{(i)} &= \sum_{k=i+1}^{n_T} \boldsymbol{h}_k x_k + \left\{ \boldsymbol{n} + \sum_{k=1}^{i} \boldsymbol{h}_k (x_k - \hat{x}_k) \right\} \\ &= \sum_{k=i+1}^{n_T} \boldsymbol{h}_k x_k + \left\{ \boldsymbol{n} + \sum_{k=1}^{i} \boldsymbol{h}_k e_k \right\} \end{aligned} \tag{4}$$

where $\boldsymbol{h}_k = [h_{1k}, h_{2k}, \ldots, h_{n_R k}]^T$ denotes the kth column vector of the channel matrix $\boldsymbol{H}$, $\hat{x}_k$ denotes the detected symbol of the kth layer, and $e_k \triangleq (x_k - \hat{x}_k)$. Note that the component $\sum_{k=1}^{i} \boldsymbol{h}_k (x_k - \hat{x}_k)$ in (4) represents the interference caused by the erroneous SIC operations due to the wrong decisions of the previously detected layers. The interference can seriously affect the system performance yet it is often assumed to be non-existent in the existing work [14–16].

To enhance the system performance, one can detect the layers in the optimal order, that is, strictly descending order of the post-detection SNR [2] of the layers. The post-detection SNR of the ith layer can be expressed as

$$\text{SNR}_i = \frac{E[|x_i|^2]}{N_0 \cdot \|\boldsymbol{w}_i\|^2} \tag{5}$$

where $\boldsymbol{w}_i$ denotes the ith row vector of the pseudo-inverse of the channel matrix $\boldsymbol{H}$. For the details of the ZF-SIC detection algorithm of VBLAST, readers please refer to [2].

3 Symbol error rate analysis

In this section, the performance of VBLAST systems employing power allocation scheme and ZF-SIC receivers with a fixed detection ordering is analysed. The analysis is carried out for both fast fading and slow Rayleigh fading channels.

3.1 Fast fading channels

Under fast fading, the channel states of consecutive symbol periods are assumed to be uncorrelated. Thus the transmitter does not have the knowledge of the channel matrix. The SER is determined by the transmitted SNR and the statistics of the fading channel gains. Denote the SER of the ith layer under power allocation pattern $\boldsymbol{K}$ and noise variance N_0 as $P\{x_i \neq \hat{x}_i \,|\, \boldsymbol{K}, N_0\}$. The SER of the ith layer has the form from [17]

$$P\{x_i \neq \hat{x}_i \,|\, \boldsymbol{K}, N_0\} = \sum_{l=0}^{i-1} P\{x_i \neq \hat{x}_i, A_{i-1}^l \,|\, \boldsymbol{K}, N_0\} \tag{6}$$

where the event A_{i-1}^l is defined as

$$A_{i-1}^l \triangleq \{\text{there exists } l \text{ detection errors in } \hat{x}_1, \ldots, \hat{x}_{i-1}\} \tag{7}$$

Let V_m denote one of the $\binom{i-1}{l}$ events which has detection errors at certain l layers among the $i-1$ processed layers. Thus V_m is one of the $\binom{i-1}{l}$ combinations of choosing l error symbols among the $i-1$ layers, where $m = 1, 2, \ldots, \binom{i-1}{l}$. We can express V_m as a set $V_m = \{v_{m,1}, v_{m,2}, \ldots, v_{m,l}\}$ where the elements of the set are indexed so that $v_{m,1} < v_{m,2} < \cdots < v_{m,l}$, $v_{m,k} \in \{1, 2, \ldots, i-1\}$. We further define its complement set as $W_m = \{1, 2, \ldots, i-1\} - V_m = \{w_{m,1}, w_{m,2}, \ldots, w_{m,i-1-l}\}$ in which the elements are also indexed with ascending order $w_{m,1} < w_{m,2} < \cdots < w_{m,i-1-l}$, $w_{m,k} \in$

IET Commun., 2010, Vol. 4, Iss. 8, pp. 956–966
doi: 10.1049/iet-com.2009.0381

$\{1, 2, \ldots, i-1\}$. Define $e^i_{V_m}$ as the event of

$$e^i_{V_m} = \Big\{x_i \neq \hat{x}_i, \cap_{\forall v_{m,k}\in V_m}\{x_{v_{m,k}} \neq \hat{x}_{v_{m,k}}\} \cap_{\forall w_{m,k}\in W_m}\{x_{w_{m,k}} = \hat{x}_{w_{m,k}}\} \,|\, \boldsymbol{K}, N_0\Big\} \tag{8}$$

Then, we have

$$P\{x_i \neq \hat{x}_i, A^l_{i-1} \,|\, \boldsymbol{K}, N_0\} = \sum_{m=1}^{\binom{i-1}{l}} P\{e^i_{V_m}\} \tag{9}$$

Moreover, we can decompose $P\{e^i_{V_m}\}$ into a product of i components following the chain rule of probability as

$$P\{e^i_{V_m}\} = P\{e^{i,i}_{V_m}\}\cdot P\{e^{i,i-1}_{V_m}\}\cdots P\{e^{i,1}_{V_m}\} = \prod_{t=1}^{i} P\{e^{i,t}_{V_m}\} \tag{10}$$

where $e^{i,t}_{V_m}$ is defined as the event of

$$e^{i,t}_{V_m} = \Big\{x_t \neq \hat{x}_t \,|\, \cap_{\forall v_{m,k}<t}\{x_{v_{m,k}} \neq \hat{x}_{v_{m,k}}\} \cap_{\forall w_{m,k}<t}\{x_{w_{m,k}} = \hat{x}_{w_{m,k}}\}, \boldsymbol{K}, N_0\Big\} \tag{11}$$

for $t \in V_m$, and

$$e^{i,t}_{V_m} = \Big\{x_t = \hat{x}_t \,|\, \cap_{\forall v_{m,k}<t}\{x_{v_{m,k}} \neq \hat{x}_{v_{m,k}}\} \cap_{\forall w_{m,k}<t}\{x_{w_{m,k}} = \hat{x}_{w_{m,k}}\}, \boldsymbol{K}, N_0\Big\} \tag{12}$$

for $t \in W_m$. Note that $\{e^{i,t}_{V_m}\}$ are not independent. For each t, the condition part of $e^{i,t}_{V_m}$ consists of the event part and the condition part of $e^{i,t-1}_{V_m}$. As the result, (9) becomes

$$P\{x_i \neq \hat{x}_i, A^l_{i-1} \,|\, \boldsymbol{K}, N_0\} = \sum_{m=1}^{\binom{i-1}{l}} \prod_{t=1}^{i} P\{e^{i,t}_{V_m}\} \tag{13}$$

Let $P_e(D, \rho)$ denote the SER of the modulation used with diversity order D in Rayleigh fading environment and transmitted SNR ρ [18, 19]. From [17, 18, 20], it is known that the diversity order of the tth layer in a VBLAST system is $D_t = n_R - n_T + t$. By approximating the effective noise, that is, the sum in the braces of (4) of the Gaussian noise and the interference from erroneous SIC operations, as a Gaussian random variable with the same variance N_t, we can have the effective SNR in tth layer as $\rho_t = E_t/N_t$. The SER of tth layer can be expressed as $P_e(D_t, \rho_t)$. From the definitions in (11) and (12), we have

$$P\{e^{i,t}_{V_m}\} = \begin{cases} P_e(n_R - n_T + t, E_t/N_t), & t \in V_m \\ 1 - P_e(n_R - n_T + t, E_t/N_t), & t \in W_m \end{cases} \tag{14}$$

Note that the value of effective noise variance N_t depends on the modulation and the symbol energy used in the previous layers. With N_t given, the SER of the ith layer, $P\{x_i \neq \hat{x}_i \,|\, \boldsymbol{K}, N_0\}$, can be computed by combining (6), (13) and (14). The average SER over all n_T layers can simply be written as

$$P_{av\,|\,(\boldsymbol{K},N_0)} = \frac{1}{n_T}\cdot\sum_{i=1}^{n_T} P\{x_i \neq \hat{x}_i \,|\, \boldsymbol{K}, N_0\} \tag{15}$$

In the following subsections, we present the expression of $P_e(D_t, \rho_t)$ and derive the effective noise variance N_t for the cases of M-QAM and M-PSK. The constellation size is denoted by M.

3.1.1 M-QAM: In this work, we only consider square M-QAM modulations such as 16-QAM, 64-QAM, and so on. The SER of tth layer using square M-QAM under Rayleigh fading can be written as follows [19]

$$P_e(D_t, \rho_t) = 4\left(1 - \frac{1}{\sqrt{M}}\right)I_1 - 4\left(1 - \frac{1}{\sqrt{M}}\right)^2 I_2 \tag{16}$$

where I_1 and I_2 are defined as

$$I_1 \triangleq \left[\frac{1}{2}\left(1 - \sqrt{\frac{\rho_t}{2/3(M-1)+\rho_t}}\right)\right]^{D_t}\cdot\sum_{k=0}^{D_t-1}\binom{D_t-1+k}{k} \times \left[\frac{1}{2}\left(1 + \sqrt{\frac{\rho_t}{2/3(M-1)+\rho_t}}\right)\right]^{k} \tag{17}$$

$$I_2 \triangleq \frac{1}{4} - \mu_t\cdot\left(\frac{1}{2} - \frac{1}{\pi}\cdot\tan^{-1}(\mu_t)\right)\cdot\sum_{k=0}^{D_t-1}\binom{2k}{k}\cdot(4\tau_t)^{-k} + \frac{\mu_t}{\pi}\sin(\tan^{-1}(\mu_t))\sum_{k=1}^{D_t-1}\sum_{i=1}^{k}\tau_t^{-k}\cdot\frac{\binom{2k}{k}}{\binom{2k}{k}4^i\cdot(2(k-i)+1)} \cdot(\cos(\tan^{-1}(\mu_t)))^{2(k-i)+1} \tag{18}$$

with

$$\mu_t = \sqrt{\frac{\rho_t}{2/3(M-1)+\rho_t}} \tag{19}$$

$$\tau_t = \left(\frac{3\rho_t}{2(M-1)} + 1\right) \tag{20}$$

Define $d_{\min}$ as the Euclidean distance between any two neighbouring M-QAM symbols in the signal space, we have $d_{\min} = \sqrt{6E_k/M-1}$. At relatively high SNR, the probability of a M-QAM symbol erroneously demodulated to another symbol with Euclidean distances greater than $d_{\min}$, is very small [18]. With such observation, we have the following approximation for the conditional pdf of e_k given $\{x_k \neq \hat{x}_k\}$

$$P_{e_k}(d_{\min}\cdot e^{j(n\pi/2)}|x_k \neq \hat{x}_k) \simeq \frac{1}{4}, \quad n = 0, 1, 2, 3 \tag{21}$$

doi: 10.1049/iet-com.2009.0381

Note that the pdf approximation implicitly ignores the cases of the transmitted M-QAM symbol locating at the edge or corner of the signal constellation. One can obtain more accurate approximation by taking the edge and corner cases into consideration. Nevertheless, numerical experiments show that the approximation above is accurate enough to capture the performance of VBLAST with M-QAM. Due to the symmetry of the pdf, it is easy to see $E[e_k \mid x_k \neq \hat{x}_k] \simeq 0$. The conditional variances is derived to be

$$\begin{aligned} \mathrm{Var}[e_k \mid \hat{x}_k \neq x_k] &= E[|e_k|^2 | \hat{x}_k \neq x_k] \\ &\simeq \frac{1}{4}(d_{\min}^2 + d_{\min}^2 + d_{\min}^2 + d_{\min}^2) \\ &= d_{\min}^2 = \frac{6}{M-1} E_k \end{aligned} \tag{22}$$

The variance N_t of the effective noise in the braces of (4) of the tth layer is thus

$$\begin{aligned} N_t &= N_0 + \sum_{\forall v_{m,k} < t} E[|h_{v_{m,k}}|^2] \cdot \mathrm{Var}[e_{v_{m,k}} \mid \hat{x}_{v_{m,k}} \neq x_{v_{m,k}}] \\ &\simeq N_0 + \frac{6}{M-1} \cdot \sum_{\forall v_{m,k} < t} E_{v_{m,k}} \end{aligned} \tag{23}$$

3.1.2 M-PSK: Using the result of [19], the SER of the tth layer using M-PSK under Rayleigh fading has the form

$$\begin{aligned} P_e(D_t, \rho_t) = & \frac{M-1}{M} - \frac{\mu_t}{\sqrt{\mu_t^2+1}} \left(\frac{1}{2} + \frac{\omega_t}{\pi} \right) \\ & \times \sum_{\tau=0}^{D_t-1} \binom{2\tau}{\tau} [4(\mu_t^2+1)]^{-\tau} - \frac{\mu_t}{\sqrt{\mu_t^2+1}} \cdot \frac{1}{\pi} \sin(\omega_t) \\ & \times \sum_{\tau=1}^{D_t-1} \sum_{i=1}^{\tau} \frac{T_{i\tau}}{(\mu_t^2+1)^\tau} [\cos(\omega_t)]^{2(\tau-i)+1} \end{aligned} \tag{24}$$

where

$$\mu_t \triangleq \sqrt{\rho_t} \sin\left(\frac{\pi}{M}\right) \tag{25}$$

$$\omega_t \triangleq \tan^{-1}\left(\frac{\sqrt{\rho_t}\cos(\pi/M)}{\sqrt{\mu_t^2+1}} \right) \tag{26}$$

$$T_{i\tau} \triangleq \frac{\binom{2\tau}{\tau}}{\binom{2(\tau-i)}{(\tau-i)} \cdot 4^i (2(\tau-i)+1)} \tag{27}$$

Following the similar argument as the M-QAM case [18], we assume that a M-PSK symbol can only be erroneously demodulated to either one of the two closest neighbouring symbols with distance $d_{\min} = 2\sqrt{E_k}\sin(\pi/M)$. The conditional pdf of e_k given $\{x_k \neq \hat{x}_k\}$ is simply

$$P_{e_k}(d_{\min} \cdot \mathrm{e}^{j(2n\pi/M)} | x_k \neq \hat{x}_k) \simeq \frac{1}{M}, \quad n = 0, 1, \ldots, M \tag{28}$$

The conditional mean is thus

$$E[e_k \mid \hat{x}_k \neq x_k] \simeq \sum_{n=0}^{M-1} \frac{1}{M} \cdot (d_{\min} \cdot \mathrm{e}^{j(2n\pi/M)}) = 0 \tag{29}$$

and the conditional variance is

$$\begin{aligned} \mathrm{Var}[e_k \mid \hat{x}_k \neq x_k] &= E[|e_k|^2 | \hat{x}_k \neq x_k] \\ &\simeq \sum_{n=0}^{M-1} \frac{1}{M} \cdot d_{\min}^2 = d_{\min}^2 \\ &= 4E_k \sin^2\left(\frac{\pi}{M}\right) \end{aligned} \tag{30}$$

The variance N_t of the effective noise in the braces of (4) of the tth layer can be expressed as

$$\begin{aligned} N_t &= N_0 + \sum_{\forall v_{m,k} < t} E[|h_{v_{m,k}}|^2] \cdot \mathrm{Var}[e_{v_{m,k}} \mid \hat{x}_{v_{m,k}} \neq x_{v_{m,k}}] \\ &\simeq N_0 + 4\sin^2\left(\frac{\pi}{M}\right) \cdot \sum_{\forall v_{m,k} < t} E_{v_{m,k}} \end{aligned} \tag{31}$$

3.2 Slow fading channel

Under slow fading, the channel remains constant for several symbols. The receiver can estimate the channel matrix $\boldsymbol{H}$ from the pilot signals and then feedback the estimated channel state information (CSI) to the transmitter. With the CSI feedback, the transmitter can supposedly find the optimal power allocation pattern to minimise the SER. In able to do so, the transmitter needs to know the SER given the CSI of $\boldsymbol{H}$, which is derived in this section.

Define $\boldsymbol{H}^{(i)}$ as the matrix whose first i column vectors are zeros and the rest column vectors are the same as $\boldsymbol{H}$ that is

$$\boldsymbol{H}^{(i)} = [\boldsymbol{0} \quad \cdots \quad \boldsymbol{0} \quad \boldsymbol{h}_{i+1} \quad \boldsymbol{h}_{j+2} \quad \cdots \quad \boldsymbol{h}_{n_\mathrm{T}}] \tag{32}$$

We further define $(\boldsymbol{H}^{(i)})^\dagger$ as the pseudo-inverse of $\boldsymbol{H}^{(i)}$, and $\boldsymbol{w}_k^{(i)}$ as the kth row of $(\boldsymbol{H}^{(i)})^\dagger$. The decision statistic $\tilde{r}_{i+1}$ of the $(i+1)$-th layer can be obtained from the received signal vector $\boldsymbol{r}^{(i)}$ of (4) following the detection

doi: 10.1049/iet-com.2009.0381

algorithm in [2]

$$
\begin{aligned}
\tilde{r}_{i+1} &= \boldsymbol{w}_{i+1}^{(i)} \cdot \boldsymbol{r}^{(i)} = \boldsymbol{w}_{i+1}^{(i)} \\
&\quad \cdot \left[\sum_{k=i+1}^{n_\mathrm{T}} \boldsymbol{h}_k x_k + \left(\boldsymbol{n} + \sum_{k=1}^{i} \boldsymbol{h}_k (x_k - \hat{x}_k) \right) \right] \\
&= x_{i+1} + \left\{ \boldsymbol{w}_{i+1}^{(i)} \cdot \boldsymbol{n} + \sum_{k=1}^{i} \boldsymbol{w}_{i+1}^{(i)} \cdot \boldsymbol{h}_k (x_k - \hat{x}_k) \right\} \\
&= x_{i+1} + \left\{ n_{i+1} + \sum_{k=1}^{i} \alpha_{i+1}^{(k)} \cdot e_k \right\}
\end{aligned} \tag{33}
$$

where $\alpha_{i+1}^{(k)} \triangleq \boldsymbol{w}_{i+1}^{(i)} \cdot \boldsymbol{h}_k$ and $n_{i+1} \triangleq \boldsymbol{w}_{i+1}^{(i)} \cdot \boldsymbol{n}$. The effective noise experienced by the $(i+1)$-th layer consists of the two terms in the brace of (33). Given the errors $e_1, e_2, \ldots, e_i$ of the previously detected layers, the effective noise of the $(i+1)$-th layer (33) is of complex Gaussian distribution with mean $\sum_{k=1}^{i} \alpha_{i+1}^{(k)} e_k$ and variance $\|\boldsymbol{w}_{i+1}^{(i)}\|^2 N_0$. To illustrate the SER derivation more efficiently, we define $\boldsymbol{e}^{(j)}$ as

$$
\boldsymbol{e}^{(j)} \triangleq [e_1,\ e_2,\ \ldots,\ e_j], \quad j = 1, 2, \ldots, n_\mathrm{T} \tag{34}
$$

The SER of the ith layer can be obtained by summing up the pdf values of all possible non-zero error realisations $\boldsymbol{\epsilon}_i$ of e_i as

$$
P\{x_i \neq \hat{x}_i \,|\, \boldsymbol{H}, \boldsymbol{K}, N_0\} = \sum_{\forall \boldsymbol{\epsilon}_i, \boldsymbol{\epsilon}_i \neq 0} P_{e_i}(\boldsymbol{\epsilon}_i \,|\, \boldsymbol{H}, \boldsymbol{K}, N_0) \tag{35}
$$

and the average SER $P_{\mathrm{av}\,|\,(\boldsymbol{H},\boldsymbol{K},N_0)}$ can be computed as

$$
P_{\mathrm{av}\,|\,(\boldsymbol{H},\boldsymbol{K},N_0)} = \frac{1}{n_\mathrm{T}} \cdot \sum_{i=1}^{n_\mathrm{T}} P\{x_i \neq \hat{x}_i \,|\, \boldsymbol{H}, \boldsymbol{K}, N_0\} \tag{36}
$$

Note that the pdf of e_i in (35) conditions on the channel matrix $\boldsymbol{H}$, power allocation pattern $\boldsymbol{K}$, and noise PSD N_0. The conditional pdf can be derived following the chain rule of probability by further conditioning on the errors observed in the previous layers $1, 2, \ldots, i-1$, which is of the following form

$$
P_{e_i}(\boldsymbol{\epsilon}_i \,|\, \boldsymbol{H}, \boldsymbol{K}, N_0) = \sum_{\forall \boldsymbol{\epsilon}_{k,k=1,\ldots,i}} \left\{ \prod_{k=1}^{i} P_{e_k}(\boldsymbol{\epsilon}_k \,|\, \boldsymbol{e}^{(k-1)}, \boldsymbol{H}, \boldsymbol{K}, N_0) \right\} \tag{37}
$$

Note that $P_{e_1}(\boldsymbol{\epsilon}_1 | \boldsymbol{e}^{(0)}, \boldsymbol{H}, \boldsymbol{K}, N_0) = P_{e_1}(\boldsymbol{\epsilon}_1 | \boldsymbol{H}, \boldsymbol{K}, N_0)$. To keep the notation simple, here we abuse the notation $\boldsymbol{e}^{(k-1)}$ by using it to denote its realisation $[\boldsymbol{\epsilon}_1, \boldsymbol{\epsilon}_2, \ldots, \boldsymbol{\epsilon}_{k-1}]$. Also note that $\boldsymbol{e}^{(k)} = [\boldsymbol{e}^{(k-1)}, \boldsymbol{\epsilon}_k]$ for each k, which is directly resulted from the chain rule.

The average SER of the whole system can thus be evaluated using (15) as long as one has the expressions of the conditional pdf's $P_{e_1}(\boldsymbol{\epsilon}_1 | \boldsymbol{H}, \boldsymbol{K}, N_0)$ and $P_{e_k}(\boldsymbol{\epsilon}_k | \boldsymbol{e}^{(k-1)}, \boldsymbol{H}, \boldsymbol{K}, N_0)$, which are derived in the following subsection for the cases of M-QAM and M-PSK.

1. *M-QAM*: Following the similar assumption in Section 3.1.1, the conditional error pdf of the first layer has the form

$$
\begin{aligned}
&P_{e_1}(d_{\min} \cdot \mathrm{e}^{j(n\pi/2)} |\, \boldsymbol{H}, \boldsymbol{K}, N_0) \\
&= \left(1 - 2\left(1 - \frac{1}{\sqrt{M}}\right) Q\left(\frac{d_{\min}/2}{\|\boldsymbol{w}_1^{(0)}\| \cdot \sqrt{N_0/2}} \right) \right) \left(1 - \frac{1}{\sqrt{M}}\right) \\
&\quad \times Q\left(\frac{d_{\min}/2}{\|\boldsymbol{w}_1^{(0)}\| \cdot \sqrt{N_0/2}} \right), \quad n = 0, 1, 2, 3
\end{aligned} \tag{38}
$$

recall $d_{\min} = \sqrt{6E_k/M - 1}$ in the case of M-QAM. The conditional error pdf of the kth layer can be further derived from (33) as

$$
\begin{aligned}
&P_{e_k}(d_{\min} \cdot \mathrm{e}^{j(n\pi/2)} | \boldsymbol{e}^{(k-1)}, \boldsymbol{H}, \boldsymbol{K}, N_0) \\
&= \left(1 - 2\left(1 - \frac{1}{\sqrt{M}}\right) Q\left(\frac{d_{\min}/2}{\|\boldsymbol{w}_k^{(k-1)}\| \cdot \sqrt{N_0/2}} \right) \right) \left(1 - \frac{1}{\sqrt{M}}\right) \\
&\quad \times Q\left(\frac{d_{\min}/2 + \Re\{\mathrm{e}^{-j(n\pi/2)} \cdot \sum_{l=1}^{k-1} \alpha_{k+1}^{(l)} \cdot e_l\}}{\|\boldsymbol{w}_k^{(k-1)}\| \cdot \sqrt{N_0/2}} \right), \\
&\quad n = 0, 1, 2, 3
\end{aligned} \tag{39}
$$

2. *M-PSK*: Following the assumption in Section 3.1.2, the conditional error pdf of the first layer is derived to be [18]

$$
\begin{aligned}
&P_{e_1}(d_{\min} \cdot \mathrm{e}^{j(2n\pi/M)} | \boldsymbol{H}, \boldsymbol{K}, N_0) = \frac{2}{M} Q\left(\frac{d_{\min}/2}{\|\boldsymbol{w}_1^{(0)}\| \sqrt{N_0/2}} \right), \\
&\quad n = 0, 1, 2, \ldots, (M-1)
\end{aligned} \tag{40}
$$

Note that for the M-PSK case, $d_{\min} = 2\sqrt{E_i}\, \sin(\pi/M)$. The conditional error pdf of the kth layer has the form of

$$
\begin{aligned}
&P_{e_k}(d_{\min} \cdot \mathrm{e}^{j(2n\pi/M)} | \boldsymbol{e}^{(k-1)}, \boldsymbol{H}, \boldsymbol{K}, N_0) \\
&= \frac{2}{M} Q\left(\frac{d_{\min}/2 - \Re\{\mathrm{e}^{-j(2n\pi/M)} \cdot (\sum_{l=1}^{k-1} \alpha_{k+1}^{(l)} \cdot e_l)\}}{\|\boldsymbol{w}_k^{(k-1)}\| \sqrt{N_0/2}} \right), \\
&\quad n = 0, 1, 2, \ldots, (M-1)
\end{aligned} \tag{41}
$$

4 Optimal power allocation

With the average SER analysed, one can find the optimal power allocation $\boldsymbol{K}$ that minimises the average SER for VBLAST systems under a given SNR. Here we demonstrate a numerical approach using Newton's method [21, 22] to find the optimal power allocation vector $\boldsymbol{K}$ that minimises the average SER $P_{\mathrm{av}\,|\,(\boldsymbol{K},N_0)}$ of the fast fading case derived in the previous section. Similar method can be applied to minimise the average SER $P_{\mathrm{av}\,|\,(\boldsymbol{H},\boldsymbol{K},N_0)}$ of the slow fading case. From our extensive numerical experiments using the brute force method, it is observed that the optimal $\boldsymbol{K}$ is generally unique. Yet, due to the complicated expression of $P_{\mathrm{av}\,|\,(\boldsymbol{K},N_0)}$, the convexity remains an open problem similarly as in the case of [13]. Nevertheless, one

doi: 10.1049/iet-com.2009.0381

can obtain the optimum usually within a few iterations of the following numerical approach.

To minimise $P_{\mathrm{av}\,|\,(\boldsymbol{K},N_0)}$, we need to find $\boldsymbol{K} = [K_1, K_2, \ldots, K_{n_\mathrm{T}-1}]$ that satisfies the following set of equations

$$\frac{\partial P_{\mathrm{av}\,|\,(\boldsymbol{K},N_0)}}{\partial K_i} = 0, \quad i = 1, \ldots, n_T - 1 \tag{42}$$

Since $P_{\mathrm{av}|(\boldsymbol{K},N_0)}$ has a very complicated form, the closed-form of its partial derivatives is even more complicated which makes it impossible to solve the equations in (42). To overcome this problem, we apply numerical approximations of $\partial P_{\mathrm{av}\,|\,(\boldsymbol{K},N_0)}/\partial K_i$ to solve for $\boldsymbol{K}$. First define

$$\begin{aligned} f_i &\triangleq \frac{\partial P_{\mathrm{av}|(\boldsymbol{K},N_0)}}{\partial K_i} \\ f_{ij} &\triangleq \frac{\partial f_i}{\partial K_j} = \frac{\partial^2 P_{\mathrm{av}|(\boldsymbol{K},N_0)}}{\partial K_i \partial K_j} \\ \boldsymbol{K}_{i+\Delta} &\triangleq (K_1, \ldots, K_i + \Delta, \ldots, K_{n_\mathrm{T}-1}) \\ \boldsymbol{K}_{i+\Delta,j+\Delta} &\triangleq (K_1, \ldots, K_i + \Delta, \ldots, K_j + \Delta, \ldots, K_{n_\mathrm{T}-1}) \end{aligned} \tag{43}$$

where $i, j \in \{1, 2, \ldots, n_\mathrm{T} - 1\}$. If Δ is chosen to be small, the partial derivatives can be closely approximated by

$$\begin{aligned} f_i &\simeq \frac{1}{\Delta}(P_{\mathrm{av}\,|\,(\boldsymbol{K}_{i+\Delta},N_0)} - P_{\mathrm{av}\,|\,(\boldsymbol{K},N_0)}) \\ f_{ij} &\simeq \frac{1}{\Delta^2}[(P_{\mathrm{av}\,|\,(\boldsymbol{K}_{i+\Delta,j+\Delta},N_0)} - P_{\mathrm{av}\,|\,(\boldsymbol{K}_{j+\Delta},N_0)}) \\ &\quad - (P_{\mathrm{av}\,|\,(\boldsymbol{K}_{i+\Delta},N_0)} - P_{\mathrm{av}\,|\,(\boldsymbol{K},N_0)})] \end{aligned} \tag{44}$$

where $i, j \in \{1, 2, \ldots, n_\mathrm{T} - 1\}$. With the approximations, we can then apply the Newton's method to solve the equations in (42). First, we start with an initial guess $\boldsymbol{K}^{(0)} = [K_1^{(0)}, K_2^{(0)}, \ldots, K_{n_\mathrm{T}-1}^{(0)}]$ and a small Δ. Then compute the associated partial derivatives $f_i^{(0)}$ and $f_{ij}^{(0)}$ from (44). For the uth iteration of the Newton's method, we define matrix $\boldsymbol{J}^{(u)}$ as

$$\boldsymbol{J}^{(u)} = \begin{bmatrix} f_{11}^{(u)} & f_{12}^{(u)} & \cdots & f_{1(n_\mathrm{T}-1)}^{(u)} \\ f_{21}^{(u)} & f_{22}^{(u)} & \cdots & f_{2(n_\mathrm{T}-1)}^{(u)} \\ \vdots & \vdots & \ddots & \vdots \\ f_{(n_\mathrm{T}-1)1}^{(u)} & f_{(n_\mathrm{T}-1)2}^{(u)} & \cdots & f_{(n_\mathrm{T}-1)(n_\mathrm{T}-1)}^{(u)} \end{bmatrix} \tag{45}$$

We further define matrix $\boldsymbol{B}_v^{(u)}$ to be the matrix obtained by replacing the vth column of $\boldsymbol{J}^{(u)}$ with $[f_1^{(u)}, f_2^{(u)}, \cdots, f_{n_\mathrm{T}-1}^{(u)}]^\mathrm{T}$. For example

$$\boldsymbol{B}_2^{(u)} = \begin{bmatrix} f_{11}^{(u)} & f_1^{(u)} & \cdots & f_{1(n_\mathrm{T}-1)}^{(u)} \\ f_{21}^{(u)} & f_2^{(u)} & \cdots & f_{2(n_\mathrm{T}-1)}^{(u)} \\ \vdots & \vdots & \ddots & \vdots \\ f_{(n_\mathrm{T}-1)1}^{(u)} & f_{n_\mathrm{T}-1}^{(u)} & \cdots & f_{(n_\mathrm{T}-1)(n_\mathrm{T}-1)}^{(u)} \end{bmatrix} \tag{46}$$

During the uth iteration, $\boldsymbol{K}^{(u+1)}$ is computed from $\boldsymbol{K}^{(u)}$ as

$$\begin{aligned} K_1^{(u+1)} &= K_1^{(u)} - \frac{|\boldsymbol{B}_1^{(u)}|}{|\boldsymbol{J}^{(u)}|} \\ K_2^{(u+1)} &= K_2^{(u)} - \frac{|\boldsymbol{B}_2^{(u)}|}{|\boldsymbol{J}^{(u)}|} \\ &\vdots \\ K_{n_\mathrm{T}-1}^{(u+1)} &= K_{n_\mathrm{T}-1}^{(u)} - \frac{|\boldsymbol{B}_{n_\mathrm{T}-1}^{(u)}|}{|\boldsymbol{J}^{(u)}|} \end{aligned} \tag{47}$$

where $|\cdot|$ denotes the matrix determinant, $u = 0, 1, \ldots$. The optimal power allocation $\boldsymbol{K}$ can be obtained by repeating the procedure until $\boldsymbol{K}^{(u)}$ converges, which generally occurs in a few iterations.

5 Power control for slow fading

In slow fading environments, the channel matrix remains constant for a certain period. As a result, power control schemes can be applied to improve the SER during the period. With the SER analysed in Section 3, we propose the optimal power control scheme and a suboptimal scheme for VBLAST systems in slow fading environments.

5.1 Optimal power control

The flowchart and the operation of the optimal power control scheme are shown in Fig. 2. Assume that the slow fading channel remains constant for L transmission periods. During the first transmission period, the transmitter has no knowledge about the current channel $\boldsymbol{H}$ and thus has to transmit using the power allocation pattern $\boldsymbol{K} = \boldsymbol{K_1}$ that minimises $P_{\mathrm{av}\,|\,(\boldsymbol{K},N_0)}$. The receiver then estimates the CSI $\hat{\boldsymbol{H}}$ and feedbacks the CSI to the transmitter. After the transmitter receives the CSI feedback from the receiver, it then uses the power allocation $\boldsymbol{K} = \boldsymbol{K_2}$ that minimises $P_{\mathrm{av}\,|\,(\hat{\boldsymbol{H}},\boldsymbol{K},N_0)}$ for the next $L-1$ transmissions. The overall operation is then repeated all over again. This optimal power control scheme can greatly improve the performance of the system, yet this is achieved at the cost of the overhead of the CSI feedback. The feedback overhead is large when the number of antennas is not small.

5.2 Suboptimal power control

Here we propose a suboptimal power control scheme which can achieve good performance with small feedback overhead.

IET Commun., 2010, Vol. 4, Iss. 8, pp. 956–966

doi: 10.1049/iet-com.2009.0381

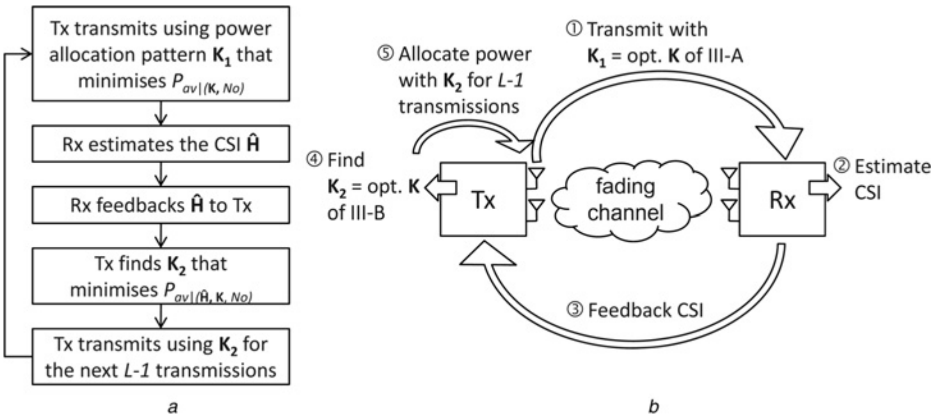

Figure 2 *Optimal power control scheme under slow fading*

The flowchart and the operation are given in Fig. 3. It is again assumed that the slow fading channel remains constant for L transmission periods. The transmitter first transmits using $\boldsymbol{K} = \boldsymbol{K}_1$ that minimises $P_{\mathrm{av}\,|\,(\boldsymbol{K},N_0)}$. The receiver then estimates the CSI $\hat{\boldsymbol{H}}$ and detects the symbols using the optimal detection ordering according to the post-detection SNR in (5). The optimal detection ordering is then sent back to the transmitter. The transmitter reorders the layers with the same layer ordering for the next $L-1$ transmission periods and transmits using the power allocation pattern $\boldsymbol{K} = \boldsymbol{K}_1$ as Step 1. The overall operation is then performed again repeatedly. With the suboptimal power control scheme, the performance degrades slightly compared with the optimal power control scheme. Yet, the receiver only feedbacks the ordering information which is of small overhead even when the number of antennas is large. Hence it is highly applicable for practical VBLAST systems.

6 Numerical results

In this section, we show the numerical results of the proposed power allocation scheme for VBLAST systems with 16-QAM and 8-PSK modulations. We first consider 4×4 VBLAST systems with 16-QAM using the proposed power allocation scheme in a fast Rayleigh fading environment. The optimal power allocation of each layer against E_b/N_0 is plotted in Fig. 4. Note that at high SNR, the impact of error propagation is more significant than the noise. The detection error in the first layer would cause serious detection problem to the following layers. As a result, we can see that K_1 increases as the SNR increases in Fig. 4.

In Fig. 5, the SER of 4×4 VBLAST systems with 16-QAM using the optimal power allocation under fast Rayleigh fading is plotted. Our SER analysis for VBLAST with power allocation is shown to be very accurate. It is observed that the proposed power allocation scheme has 4 dB gain at SER around 10^{-4} comparing to the original VBLAST without power allocation. This shows the superior performance of the proposed power allocation scheme.

We then consider 4×4 VBLAST systems with 8-PSK under fast fading. The optimal power allocation patterns against E_b/N_0 are plotted in Fig. 6. In this figure, we can see that K_1 increases as the SNR increases, just like in the case of 16-QAM. The SER curves of 4×4 VBLAST systems with 8-PSK are plotted in Fig. 7. In this figure, the average SER analysis results closely follow the simulation results. The VBLAST systems with 8-PSK

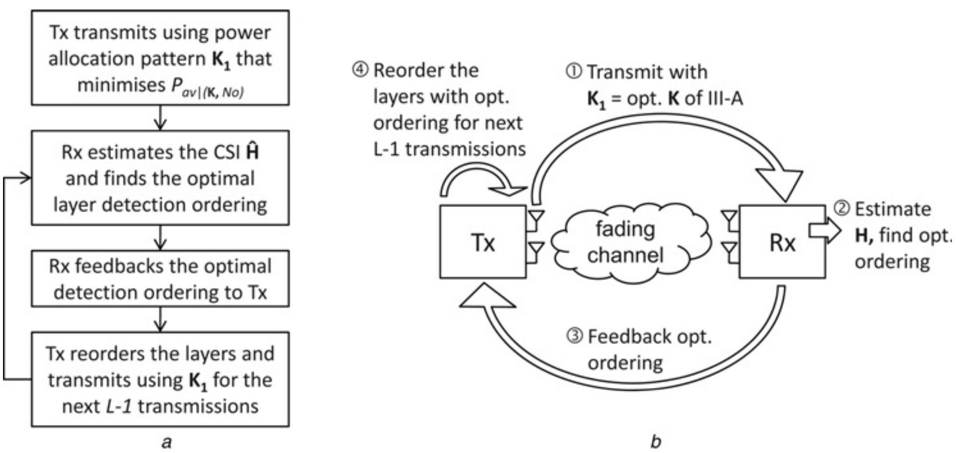

Figure 3 *Suboptimal power control scheme under slow fading*

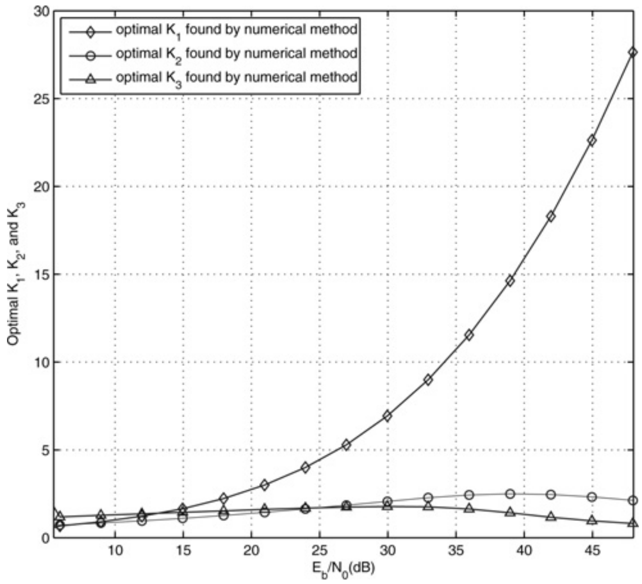

Figure 4 *Optimal power allocation* $\mathbf{K} = [K_1, K_2, K_3]$ *for 4 × 4 VBLAST systems with 16-QAM under fast Rayleigh fading*

using the optimal power allocation have signal gains ranging from 3.5 to 4 dB compared to the original VBLAST systems without power allocation. The SER of layers 1 and 4 is also plotted in Figs. 5 and 7. It is observed that the layer SER has much smaller variation among the layers of the VBLAST systems with power allocation than the original VBLAST systems without power allocation. This is another merit of the proposed power allocation scheme.

For the slow fading case, we plot the SER curves of 4 × 4 VBLAST systems with 16-QAM using the optimal and suboptimal power control schemes in Fig. 8, respectively. The simulation is conducted by regenerating the channel state matrix every 10 transmissions. In Fig. 8, it is observed that the optimal power allocation scheme outperforms the original VBLAST system by 10 dB for 4 × 4 VBLAST with 16-QAM. The optimal power allocation scheme significantly improves the SER performance at the cost of the large CSI feedback overhead. To reduce the overhead, we consider the use of the suboptimal power control scheme and the resulting SNR gain is 8.5 dB for 4 × 4 VBLAST with 16-QAM. The suboptimal power control scheme offers a good

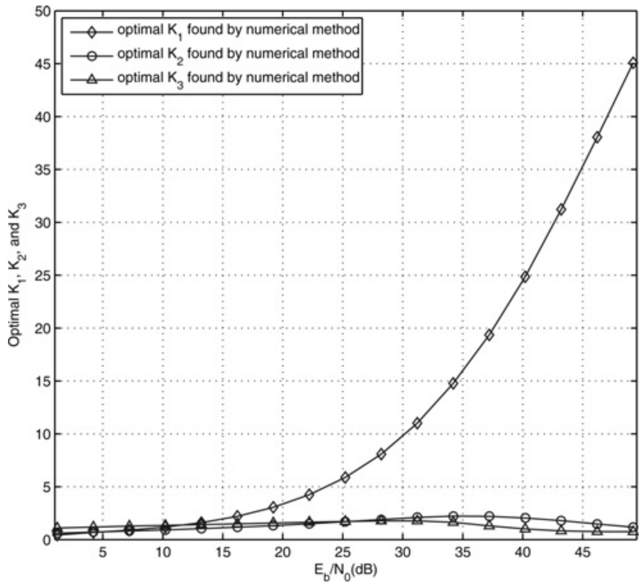

Figure 6 *Optimal power allocation* $\mathbf{K} = [K_1, K_2, K_3]$ *for 4 × 4 VBLAST systems with 8-PSK under fast Rayleigh fading*

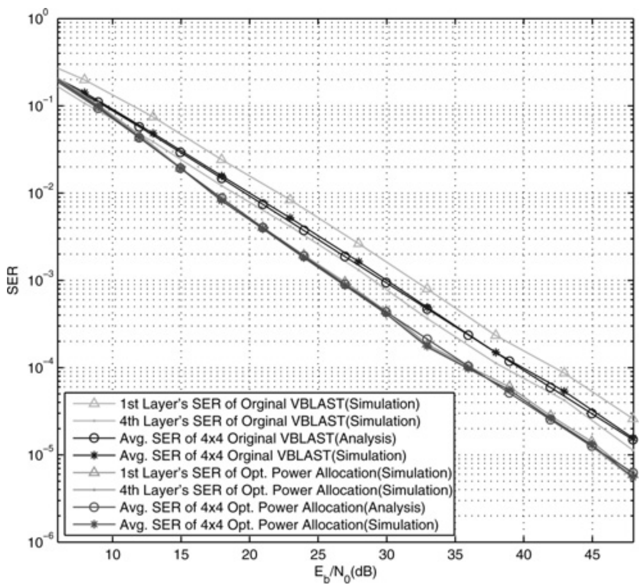

Figure 5 *Symbol error rate of 4 × 4 VBLAST systems with 16-QAM using the optimal power allocation under fast Rayleigh fading*

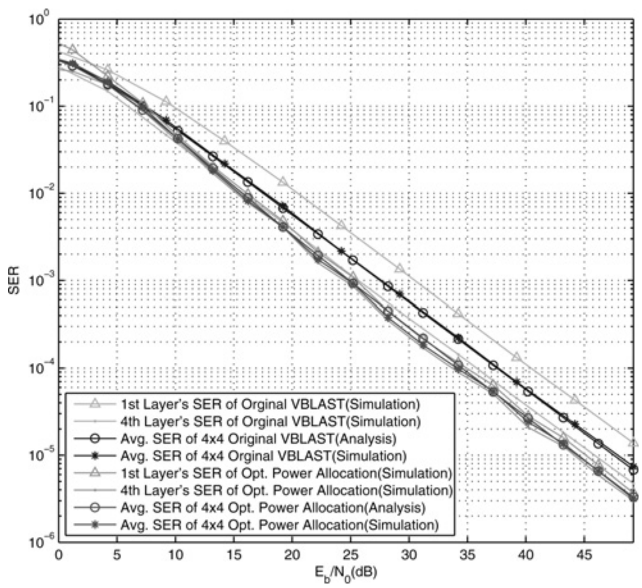

Figure 7 *Symbol error rate of 4 × 4 VBLAST systems with 8-PSK using the optimal power allocation under fast Rayleigh fading*

doi: 10.1049/iet-com.2009.0381

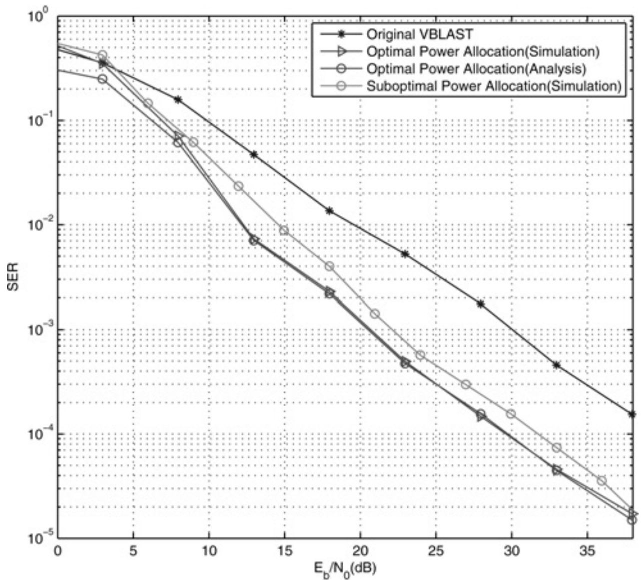

Figure 8 *Symbol error rate of 4 × 4 VBLAST systems with 16-QAM using the optimal/suboptimal power control schemes under slow Rayleigh fading*

balance between the SER performance and the feedback overhead. Note that both optimal and suboptimal power control schemes in the slow fading case have larger gains than the case of fast fading. The relatively larger gains in the slow fading case are resulted from the use of CSI or detection ordering feedback information at the transmitter to improve the system performance. Whereas, in the case of fast fading, such feedback information is not available at the transmitter.

7 Conclusions

In this paper, we have proposed a power allocation scheme for VBLAST systems with M-ary modulations employing ZF-SIC detection over both fast and slow Rayleigh fading channels. The proposed power allocation scheme optimally allocates power to the VBLAST layers by analytically minimising the SER of the VBLAST systems. The average SER expressions of VBLAST systems employing M-PSK and M-QAM in fast and slow fading environments have been derived with error propagation effect among the layers taken into consideration. Numerical optimisation method has been applied to find the optimal power allocation that minimises the average SER. Simulations have shown that our SER analysis is accurate and the proposed power allocation scheme provides significant SNR gain of 3.5–4 dB in fast fading environments. The proposed power allocation scheme is also shown to be very effective in reducing the variation of the layer SER. The proposed power allocation scheme has also been applied to the power control of VBLAST systems in slow fading environments. Significant SNR gains of 8.5–10 dB have been observed in the numerical experiments.

8 Acknowledgment

This work was supported in part by the Excellent Research Projects of National Taiwan University under Contract 97R0062-06, by the National Science Council (ROC) under Contract NSC98-2220-E-002-005, and by KFUPM under grant number FT040009.

9 References

[1] FOSCHINI G.J.: 'Layered space-time architecture for wireless communication in a fading environment when using multiple antennas', *Bell Labs Tech. J.*, 1996, **1**, (2), pp. 41–59

[2] WOLNIANSKY P.W., FOSCHINI G.J., GOLDEN G.D., VALENZUELA R.A.: 'V-blast: an architecture for realizing very high data rates over the rich-scattering wireless channel'. Proc. ISSSE, 1998, pp. 295–300

[3] WANG N., BLOSTEIN S.D.: 'Approximate minimum ber power allocation for mimo spatial multiplexing systems', *IEEE Trans. Commun.*, 2006, **54**, (12), pp. 2212–2212

[4] LOYKA S., GAGNON F.: 'Performance analysis of the v-blast algorithm: an analytical approach', *IEEE Trans. Wirel. Commun.*, 2004, **3**, (4), pp. 1326–1337

[5] NAM S.H., LEE K.B.: 'Transmit power allocation for an extended v-blast system', *Personal, Indoor Mobile Radio Commun.*, 2002, **2**, pp. 843–848

[6] KALBASI R., FALCONER D.D.: 'Optimum power allocation for a v-blast system with two antennas at the transmitter', *IEEE Commun. Lett.*, 2005, **9**, (9), pp. 826–828

[7] LI Y., SOONG A.C.K., LU J., DU Y.: 'Power allocation without csi feedback for decision-feedback mimo signal detection'. IEEE Wireless Communications and Networking Conf., Hong Kong, March 2007, pp. 1119–1123

[8] PRASAD N., VARANASI M.K.: 'Analysis of decision feedback detection for mimo rayleigh-fading channels and the optimization of power and rate allocations', *IEEE Trans. Inform. Theory*, 2004, **50**, (6), pp. 1009–1025

[9] CHOI J.: 'Nulling and cancellation detector for mimo channels and its application to multistage receiver for coded signals: Performance and optimization', *IEEE Trans. Wirel. Commun.*, 2006, **5**, (5), pp. 1207–1216

[10] ZHONGPENG W.: 'A group iterative qr receiver based on flat mimo channels'. Int. Conf. on Wireless Communications, Networking and Mobile Computing, 2007

[11] CHEN H.-Y., CHUANG C.-H., YEH P.-C.: 'Power diversity scheme for v-blast systems under rayleigh fading'. IEEE Vehicular Technology Conf., Singapore, May 2008, pp. 534–538

[12] CHUANG C.-H.: 'Power diversity for mimo systems with v-blast detection'. Master's thesis, Graduate Institute of Communication Engineering, National Taiwan University, Taipei, Taiwan, June 2007

[13] KOSTINA V., LOYKA S.: 'On optimum power allocation for the v-blast', *IEEE Trans. Commun.*, 2008, **56**, (6), pp. 999–1012

[14] DOOSTNEJAD R., LIM T.J., SOUSA E.S.: 'Impact of power control on the performance of space-time spreading systems with suboptimal detectors', *Commun. Comput. Signal Process.*, 2003, **1**, pp. 506–509

[15] MIZHOU T., BAR-NESS Y.: 'Optimal power distribution control under different total power constraint strategies for multicode mc-cdma with zero-forcing successive interference cancellation'. IEEE Wireless Communications and Networking Conf., 21–25 March 2004, vol. 3, pp. 1376–1381

[16] TAN M., BAR-NESS Y.: 'Equal ber power control for uplink mc-cdma with mmse successive interference cancellation', *IEEE Commun. Lett.*, 2004, **8**, (6), pp. 348–350

[17] SHEN C., ZHU Y., ZHOU S., JIANG J.: 'On the performance of v-blast with zero-forcing successive interference cancellation receiver'. Proc. IEEE Global Telecommunications Conf., 29 November–3 December 2004, vol. 5, pp. 2818–2822

[18] PROAKIS J.G.: 'Digital communications' (McGraw-Hill, 2001, 4th edn.)

[19] AL-SHAHLAN F.F.: 'Performance analysis of mqam nakagami fading channels'. PhD dissertation, King Fahd University of Petroleum and Minerals, Dhahran, Saudi Arabia, 2000

[20] LOYKA S., GAGNON F.: 'Performance analysis of the v-blast algorithm: an analytical approach'. Proc. Int. Zurich Seminar on Broadband Communications, February 2002

[21] GERALD C.F., WHEATLEY P.O.: 'Applied numerical analysis' (Addison Wesley, 2003, 6th edn.)

[22] LUENBERGER D.G.: 'Linear and nonlinear programming' (Addison Wesley, 1986, 2nd edn.)

doi: 10.1049/iet-com.2009.0381